 CMES, vol.95, no.6, pp.519-534, 2013

# Interactions of Three Parallel Square-Hole Cracks in an Infinite Plate Subjected to Internal Pressure

**Changqing Miao**[1], **Yintao Wei**[2] **and Xiangqiao Yan**[1]

**Abstract:** By using a hybrid displacement discontinuity method, the interactions of three parallel square-hole cracks in an infinite plate subjected to internal pressure are investigated in this paper. Numerical examples are included to illustrate that the numerical approach is very simple and effective for calculating the stress intensity factors (SIFs) of complex plane crack problems. Many numerical results of the SIFs are given and discussed. It is found that a square hole has a shielding effect on crack(s) emanating from the hole. The finding perhaps has an important meaning in engineering.

**Keywords:** Parallel Cracks, Square hole, Stress intensity factor, Crack-tip element, Displacement discontinuity method.

## 1 Introduction

Due to the stress concentration effect around the hole, cracks are likely to initiate at the hole under the action of fatigue loading. Consequently, a number of papers dealing with hole edge crack problems are available. For radial crack(s) emanating from a circular hole in an infinite plate under tension, typical solutions were given by Bowie (1956) and by Newman (1971). For radial cracks emanating from an elliptical hole in an infinite plate under tension, typical solutions were obtained by Nisitani and Isida (1982), by Murakami (1978) by using the body force and by Newman (1971) by using the boundary collocation method. For cracks emanating from a triangular or square hole in an infinite plate under tension, Murakami (1978) used the body force method to calculate their stress intensity factors.

The boundary element method (BEM) also known a boundary integral equation (BIE) method has proven to be a robust and accurate numerical technique in many engineering disciplines. The attraction of BEM can be largely attributed to the reduction in the dimensionality of the problem; for 2D analysis only the line bound-

[1] Res Lab on Composite Materials, Harbin Inst Technol, Harbin, 150001, P.R.China.
[2] Dept Automot Engn, Tsinghua University, Beijing, 100084, P. R China.

ary of the domain needs to be discretized into elements and for 3D problems only the surface of the domain needs to be discretized. This means that, compared to domain type analysis, a boundary analysis results in a substantial reduction in data preparation and a much smaller system of equations to be solved. Furthermore, this simpler description of the body means that regions of high stress concentration can be modeled more efficiently as the necessary high concentration of grid points in confined to one less dimension. The ability of model high stress gradients accurately and efficiently has been the main reason for the method success in fracture mechanics applications [e.g., Aliabadi (1997); Dong and Atluri (2012); Dong and Atluri (2013a,b); Cruse (1972)]. Indeed, fracture mechanics has been the most active specialized area of research in the boundary element method and probably the one most exploited by industry.

Various formulations of boundary integral equation methods have been developed for elastic fracture mechanics problems. These formulations differ from each other mainly because of the different approaches used in dealing with the singularity of stress near a crack tip and the geometry identity of the surfaces of a crack. The standard boundary element formulation, when regarding the cracks as narrow slits with upper and lower surfaces slightly separated, degenerates for flat cracks and is simply not appropriate for numerical modeling [e.g, Cruse (1972)]. This degeneracy is linked to the ill-posed nature of problems with two coplanar surfaces. Several different formulations have been proposed to avoid this fundamental limitation. The first one is the Green's function method by Cruse (1978), which has the advantage of avoiding crack surface modeling and gives excellent accuracy. It is however restricted to fracture problems involving very simple crack geometries for which analytical Green's functions can be obtained. The second one is the multi-domain technique by Blandford, Ingraffea and Liggett (1981). The advantage of this approach is its ability to model cracks with any geometric shape. The disadvantage is an artificial subdivision of the original domain into several subdomains, thus resulting in a large system of equations. The third approach is the displacement discontinuity method by Crouch and Starfied (1983). Instead of using the Green's displacements and stresses from point forces, the displacement discontinuity method uses Greens functions corresponding to point dislocations (i.e., displacement discontinuity). The fourth approach is the so-called Dual Boundary Element Method [e.g., Portela, Aliabadi and Rook (1992); Mi and Aliabadi (1992); Leonel and Venturini (2010); Wang and Yao (2011)] where the displacement integral equation is collocated on the no-crack boundary and on one side of the crack surface while the traction integral equation is collocated on the other side of the crack surface. For each formulation, in order to model the singularity of stress near a crack tip, options are available such as building in the crack-tip stress singularity [e.g., Tanaka, and

Itoh (1987); Kebir, Roelandt and Foulquier (1999)], using the quarter-point boundary element by Blandford, Ingraffea and Liggett (1981), and strategically refining the near-crack-tip nonsingular element. Further details on elastic crack analysis by the boundary element method are given by Aliabadi (1997) and Cruse (1989).

In addition, the displacement discontinuity method are more straight-forward when dealing with infinite domains. For practical problems with finite domains, the alternating method by SN Atluri and co-workers [Park and Atluri (1998); Dong and Atluri (2013b)] can be combined with the displacement discontinuity method. The displacement-discontinuity method can be used to model cracks in an infinite domain, with the coarse FEM can be used to model finite structures without considering the cracks.

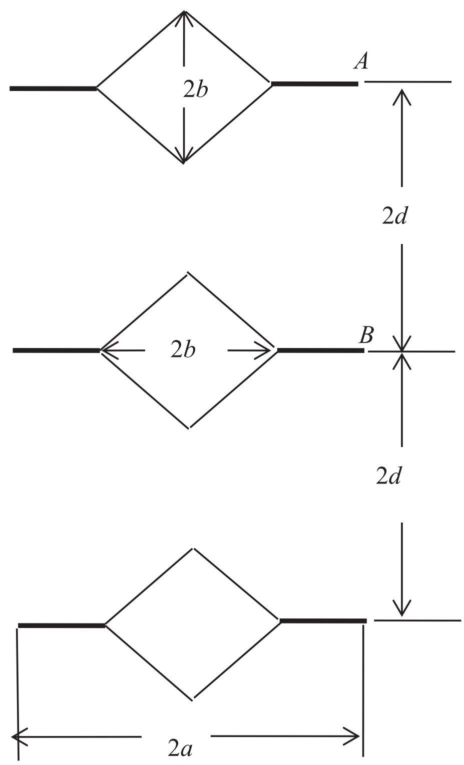


Figure 1: Schematic of three parallel square-hole cracks in an infinite plate subjected to internal pressure $p$ (internal pressure$p$ on hole faces and crack faces is not pictured)

By using a hybrid displacement discontinuity method, the interactions of three parallel square-hole cracks in an infinite plate subjected to internal pressure shown in Fig.1 are investigated in this paper. It is found that the previous investigations that the hybrid displacement discontinuity method has very high accuracy and efficiency for a branched crack [e.g. Yan (2004a); Yan (2005a); and Yan (2006a)], complex plane cracks in a finite plate (2004b; 2005b and 2006b), a multiple cracks interaction [e.g., Yan (2003a); Yan (2005c) and Yan (2006e)], a mixed-mode crack problem [e.g., Yan (2006d)], including a fatigue growth simulation of a mixed-mode crack [e.g., Yan (2006e)]. In this paper, numerical examples are given to illustrate that the numerical approach is very simple and effective for calculating the stress intensity factors (SIFs) of complex plane crack problems. Many numerical results are given and discussed. It is found that a square hole has a shielding effect on crack(s) emanating from the hole. The finding perhaps has an important meaning in engineering.

## 2 Description of the Hybrid Displacement Discontinuity Method

In this section, the hybrid displacement discontinuity method presented by Yan (2005b) is described briefly. It consists of the constant displacement discontinuity element presented by Crouch and Starfield (1983) and the crack-tip displacement discontinuity elements.

### *2.1 Constant Displacement Discontinuity Element*

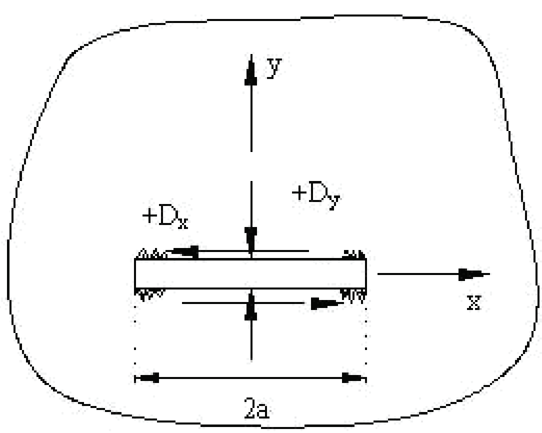


Figure 2: Schematic of constant displacement discontinuity components $D_x$ and $D_y$

The displacement discontinuity $D_i$ is defined as the difference in displacement between the two sides of the segment (see Fig.2):

$$\begin{aligned} D_x &= u_x(x,0_-) - u_x(x,0_+) \\ D_y &= u_y(x,0_-) - u_y(x,0_+) \end{aligned} \tag{1}$$

The solution to the subject problem is given by Crouch and Starfield (1983). The displacements and stresses can be written as

$$\begin{aligned} u_x &= D_x[2(1-\nu)F_3(x,y) - yF_5(x,y)] + D_y[-(1-2\nu)F_2(x,y) - yF_4(x,y)], \\ u_y &= D_x[(1-2\nu)F_2(x,y) - yF_4(x,y)] + D_y[2(1-\nu)F_3(x,y) - yF_5(x,y)], \end{aligned} \tag{2}$$

and

$$\begin{aligned} \sigma_{xx} &= 2GD_x[2F_4(x,y) + yF_6(x,y)] + 2GD_y[-F_5(x,y) + yF_7(x,y)], \\ \sigma_{yy} &= 2GD_x[-yF_6(x,y)] + 2GD_y[-F_5(x,y) - yF_7(x,y)], \\ \sigma_{xy} &= 2GD_x[-F_5(x,y) + yF_7(x,y)] + 2GD_y[-yF_6(x,y)]. \end{aligned} \tag{3}$$

$G$ and $\nu$in these equations are shear modulus and Poisson's ratio, respectively. Functions $F_2$ through $F_7$ are described by Crouch and Starfield (1983). Eqs (2) and (3) are used by Crouch and Starfield (1983) to set up a constant displacement discontinuity method.

### *2.2 Crack-Tip Displacement Discontinuity Elements*

By using the Eqs (2) and (3), recently, Yan (2005b) presented crack-tip displacement discontinuity elements, which can be classified as the left and the right crack-tip displacement discontinuity elements to deal with crack problems in general plane elasticity. The following gives basic formulas of the left crack-tip displacement discontinuity element.

For the left crack-tip displacement discontinuity element (see Fig.3), its displacement discontinuity functions are chosen as

$$D_x = H_s\left(\frac{a_{tip}+\xi}{a_{tip}}\right)^{\frac{1}{2}}, \qquad D_y = H_n\left(\frac{a_{tip}+\xi}{a_{tip}}\right)^{\frac{1}{2}}. \tag{4}$$

where $H_s$ and $H_n$ are the tangential and normal displacement discontinuity quantities at the center of the element, respectively, $a_{tip}$ is a half length of crack-tip element. Here, it is noted that the element has the same unknowns as the two-dimensional constant displacement discontinuity element. But it can be seen that the displacement discontinuity functions defined in (4) can model the displacement fields around the crack tip. The stress field determined by the displacement discontinuity functions (4) possesses $r^{-1/2}$ singularity around the crack tip.

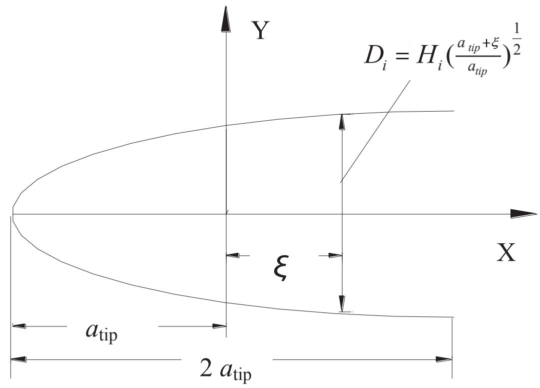


Figure 3: Schematic of the left crack tip displacement discontinuity element

Based on the Eqs (2) and (3), the displacements and stresses at a point $(x,y)$ due to the left crack-tip displacement discontinuity element can be obtained,

$$\begin{aligned} u_x &= H_s[2(1-\nu)B_3(x,y) - yB_5(x,y)] + H_n[-(1-2\nu)B_2(x,y) - yB_4(x,y)], \\ u_y &= H_s[(1-2\nu)B_2(x,y) - yB_4(x,y)] + H_n[2(1-\nu)B_3(x,y) - yB_5(x,y)], \end{aligned} \tag{5}$$

and

$$\begin{aligned} \sigma_{xx} &= 2GH_s[2B_4(x,y) + yB_6(x,y)] + 2GH_n[-B_5(x,y) + yB_7(x,y)], \\ \sigma_{yy} &= 2GH_s[-yB_6(x,y)] + 2GH_n[-B_5(x,y) - yB_7(x,y)], \\ \sigma_{xy} &= 2GH_s[-B_5(x,y) + yB_7(x,y)] + 2GH_n[-yB_6(x,y)], \end{aligned} \tag{6}$$

where functions $B_2$ through $B_7$ are described by Yan (2005b).

### *2.3 Implementation of the Hybrid Displacement Discontinuity Method*

Crouch and Starfield (1983) used Eqs (2) and (3) to set up constant displacement discontinuity boundary element equations. Similarly, we can use Eqs (5) and (6) to set up boundary element equations associated with the crack-tip elements. The constant displacement discontinuity element together with the crack-tip elements is combined easily to form a very effective numerical approach for calculating the SIFs of general plane cracks. In the boundary element implementation, the left or the right crack-tip element is placed locally at the corresponding left or right crack tip on top of the constant displacement discontinuity elements that cover the entire crack surface and the other boundaries. The method is called a hybrid displacement discontinuity method (HDDM).

### 2.4 Computational Formulas of the Stress Intensity Factors

The objective of many analyses of linear elastic crack problems is to obtain the SIFs $K_I$ and $K_{II}$. Based on the displacement field around the crack tip, the following formulas exist

$$K_I = -\frac{\sqrt{2\pi}GH_n}{4(1-\nu)\sqrt{a_{tip}}}, \qquad K_{\mathrm{II}} = -\frac{\sqrt{2\pi}GH_s}{4(1-\nu)\sqrt{a_{tip}}}. \tag{7}$$

### 2.5 A Numerical Example

In order to illustrate the accuracy and efficiency of the hybrid displacement discontinuity method for analyzing crack problems, an example is given here.

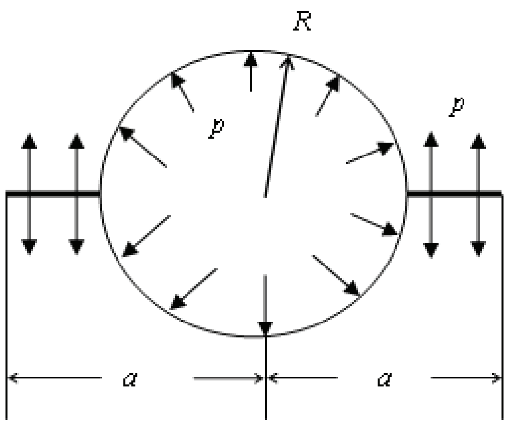


Figure 4: Schematic of a circular-hole crack in an infinite plate subjected to internal pressure $p$.

Shown in Fig.4 is a circular-hole crack in an infinite plate subjected to internal pressure $p$. For this problem, the symmetric conditions can be used. The following cases are considered

$a/R = 1.02, 1.04, 1.06, 1.08, 1.10, 1.15, 1.2, 1.25, 1.3, 1.4, 1.5, 1.6, 1.8, 2.0, 2.2, 2.5, 3.0$

Regarding discretization, here, the number of elements on a quarter of the circular hole is 200 and the other boundaries are discretized according to the limitation that all boundary elements have approximately the same length. The calculated SIFs normalized by $p\sqrt{\pi a}$ are given in Table 1. For the comparison purpose, Table 1 also lists the numerical result reported by Bowie (1956). From Table 1, it is found that the calculated results are in excellent agreement with those reported by Bowie (1956).

Table 1: Normalized SIFs of a circular-hole crack in an infinite plate subjected to internal pressure.

| $a/R$ | present | Bowie (1956) |
|---|---|---|
| 1.02 | 0.2963 | 0.3058 |
| 1.04 | 0.4123 | 0.4183 |
| 1.06 | 0.4915 | 0.4958 |
| 1.08 | 0.5517 | 0.5551 |
| 1.10 | 0.5999 | 0.6025 |
| 1.15 | 0.6878 | 0.6898 |
| 1.20 | 0.7479 | 0.7494 |
| 1.25 | 0.7916 | 0.7929 |
| 1.30 | 0.8247 | 0.8259 |
| 1.40 | 0.8711 | 0.8723 |
| 1.50 | 0.9016 | 0.9029 |
| 1.60 | 0.9228 | 0.9242 |
| 1.80 | 0.9496 | 0.9513 |
| 2.00 | 0.9651 | 0.9670 |
| 2.20 | 0.9747 | 0.9768 |
| 2.50 | 0.9832 | 0.9855 |
| 3.00 | 0.9899 | 0.9927 |

## 3 Numerical Results and Discussions

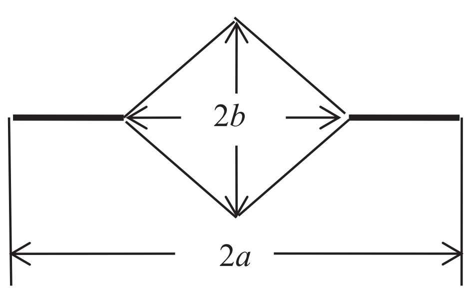


Figure 5: Schematic of a square-hole crack in an infinite plate subjected to internal pressure $p$ (internal pressure $p$ is not pictured).

Table 2: Normalized SIFs of a square-hole crack in an infinite plate subjected to internal pressure $p$.

| $a/b$ | 1.005 | 1.01 | 1.02 | 1.04 | 1.06 | 1.08 | 1.10 | 1.15 | 1.29 | 1.25 | 1.30 |
|---|---|---|---|---|---|---|---|---|---|---|---|
| SIFs | 0.7546 | 0.7794 | 0.8046 | 0.8314 | 0.8482 | 0.8603 | 0.8705 | 0.8907 | 0.9051 | 0.9161 | 0.9261 |
| $a/b$ | 1.35 | 1.50 | 2.0 | 2.5 | 3.0 | 3.5 | 4.0 | 4.5 | 5.0 | 10.0 | |
| SIFs | 0.9339 | 0.9523 | 0.9811 | 0.9918 | 0.9956 | 0.9973 | 0.9980 | 0.9984 | 0.9986 | 0.9984 | |

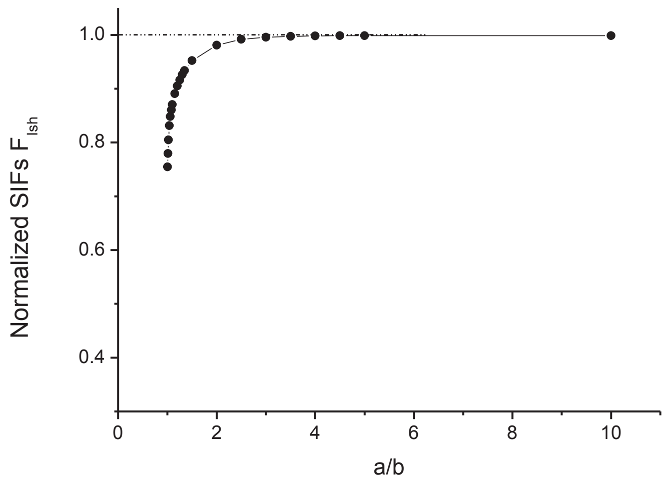


Figure 6: Normalized SIFs of a square-hole crack in an infinite plate subjected to internal pressure $p$.

Before analyzing three parallel square-hole cracks in an infinite plate subjected to internal pressure $p$ shown in Fig.1, first a square-hole crack in an infinite plate subjected to internal pressure $p$ shown in Fig.5 is studied by using the hybrid displacement discontinuity method. Here, the SIFs of the square-hole crack are expressed mathematically as $K_{Ish}(a/b)$. If the SIFs of the center crack of the length $2a$ subjected to internal pressure $p$ are expressed as $K_{Icc}$, then their ratio can be denoted by $F_{Ish}$

$$F_{Ish} = K_{Ish}(a/b)/K_{Icc} = K_{Ish}(a/b)/(p\sqrt{\pi a}) \tag{8}$$

which is called a normalized SIFs. The calculated normalized SIFs $F_{Ish}$ are given in Table 2, also see Fig.6. From Fig.6, it can be seen that:

With an increase of $a_b(=a/b)$, $F_{Ish}$ fast increases monotonously and subsequently increases slowly. As $a_b$ are large enough (e.g. $a_b \succ a_{bl}$), $F_{Ish}$ reaches its maximum

$F_{Ishm}$, and keeps this maximum with an increase of $a_b$. Here, $a_{bl} = 2.50$, $F_{Ishm} = 1$. After introducing the dimensionless parameters,$a_{bl}$and$F_{Ishm}$, it is found that:

(1) As $a_b < a_{bl}$, a square hole has a **shielding effect** on the cracks emanating from the hole. And the closer the size of the square hole is to that of the crack, the stronger the shielding effect is.

(2) As $a_b > a_{bl}$, a square hole has no effect on the SIFs of the cracks emanating from the hole. That is to say that at this time the size of the square hole is small enough relative to that of the center crack, the effect of the square hole on the SIFs of cracks emanating from the hole is completely neglected.

The interactions of three parallel square-hole cracks in an infinite plate subjected to internal pressure $p$ shown in Fig.1 are investigated by using the hybrid displacement discontinuity method. The following cases are considered,

$$a/b = 1.01, 1.02, 1.04, 1.06, 1.08, 1.10, 1.15, 1.25, 1.50, 2.50, 4.00$$
$$a/d = 0.05, 0.20, 0.40, 0.70, 0.80, 0.84, 0.88, 0.90$$

For the hole crack problem shown in Fig.1, the symmetry conditions can be used. Thus its quarter boundary is discretized in the boundary element analysis. Regarding discretizations, number of elements (denoted by $N$) on a branched crack is given in Table 3, the other boundaries are discretized according to the limitation that all boundary elements have approximately the same length.

If the SIFs normalized by $p\sqrt{\pi a}$ for three parallel square-hole cracks are denoted by $F_{Ithcp}$, obviously, $F_{Ithcp}$ can be expressed mathematically as

$$F_{Ithcp} = F_{Ithcp}(a/b, a/d) \tag{9}$$

If we let the SIFs normalized by $p\sqrt{\pi a}$ for three parallel cracks with same length in an infinite plate subjected to internal pressure $p$ be denoted by $F_{Itcp}$, then $F_{Itcp}$ can be expressed mathematically as

$$F_{Itcp} = F_{Itcp}(a/d) \tag{10}$$

The calculated SIFs $F_{Ithcp}$ are given in Tables 4 and 5. The SIFs $F_{Itcp}$ reported by Isida (1976) are listed in Table 6. It can be seen from Tables 2, 4, 5 and 6 that:

(1) When $a/d$ is very small, for example, $a/d = 0.05$, the interactions of three parallel square-hole cracks can be neglected. At this time, the SIFs $F_{Ithcp}$ at the crack tips $A$ and $B$ are all almost equal and equal to those of single square-hole crack $F_{Ish}$.

(2) When $a/b$ is large enough, for example, $a/b = 4.00$, the effect of square holes on the SIFs can be neglected. At this time, the SIFs $F_{Ithcp}$ at the crack tip $A$ for three

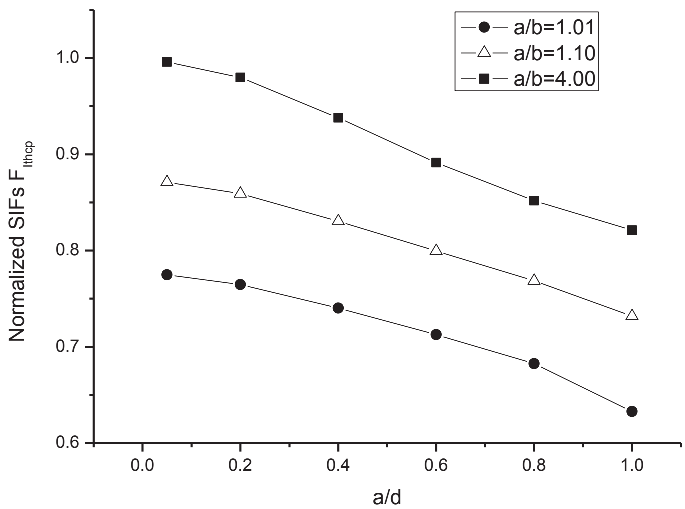


Figure 7: Normalized SIFs $F_{Ithcp}$ at the crack tip $A$ for three parallel square-hole cracks in an infinite plate subjected to internal pressure.

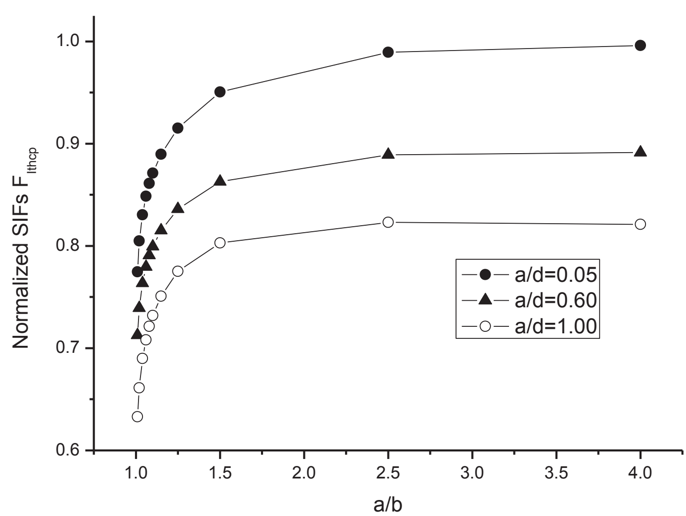


Figure 8: Normalized SIFs $F_{Ithcp}$ at the crack tip A for three parallel square-hole cracks in an infinite plate subjected to internal pressure .

Table 3: Number of elements on a branched crack for the crack problem shown in Fig.1

| a/b | 1.01 | 1.02 | 1.04 | 1.06 | 1.08 | 1.10 | 1.15 | 1.25 | 1.50 | 2.50 | 4.00 |
|---|---|---|---|---|---|---|---|---|---|---|---|
| $N$ | 3 | 5 | 5 | 7 | 10 | 10 | 20 | 25 | 50 | 150 | 300 |

Table 4: Normalized SIFs of crack tip $A$ for three parallel square-hole cracks in an infinite plate subjected to internal pressure

| a/d | a/b | | | | | | | | | | |
|---|---|---|---|---|---|---|---|---|---|---|---|
| | 1.01 | 1.02 | 1.04 | 1.06 | 1.08 | 1.10 | 1.15 | 1.25 | 1.50 | 2.50 | 4.00 |
| 0.05 | 0.7747 | 0.8048 | 0.8304 | 0.8486 | 0.8612 | 0.8711 | 0.8897 | 0.9153 | 0.9505 | 0.9894 | 0.9960 |
| 0.20 | 0.7647 | 0.7936 | 0.8197 | 0.8370 | 0.8496 | 0.8592 | 0.8775 | 0.9022 | 0.9362 | 0.9735 | 0.9797 |
| 0.40 | 0.7401 | 0.7677 | 0.7930 | 0.8096 | 0.8215 | 0.8305 | 0.8476 | 0.8702 | 0.9008 | 0.9332 | 0.9379 |
| 0.60 | 0.7127 | 0.7394 | 0.7637 | 0.7796 | 0.7908 | 0.7994 | 0.8153 | 0.8360 | 0.8628 | 0.8891 | 0.8913 |
| 0.80 | 0.6825 | 0.7082 | 0.7325 | 0.7485 | 0.7598 | 0.7686 | 0.7847 | 0.8052 | 0.8306 | 0.8519 | 0.8517 |
| 1.00 | 0.6329 | 0.6612 | 0.6900 | 0.7082 | 0.7213 | 0.7320 | 0.7508 | 0.7751 | 0.8030 | 0.8231 | 0.8212 |

Table 5: Normalized SIFs of crack tip $B$ for three parallel square-hole cracks in an infinite plate subjected to internal pressure

| a/d | a/b | | | | | | | | | | |
|---|---|---|---|---|---|---|---|---|---|---|---|
| | 1.01 | 1.02 | 1.04 | 1.06 | 1.08 | 1.10 | 1.15 | 1.25 | 1.50 | 2.50 | 4.00 |
| 0.05 | 0.7745 | 0.8033 | 0.8302 | 0.8478 | 0.8606 | 0.8704 | 0.8892 | 0.9146 | 0.9499 | 0.9888 | 0.9954 |
| 0.20 | 0.7582 | 0.7864 | 0.8125 | 0.8297 | 0.8420 | 0.8515 | 0.8695 | 0.8937 | 0.9270 | 0.9633 | 0.9693 |
| 0.40 | 0.7166 | 0.7430 | 0.7674 | 0.7833 | 0.7946 | 0.8031 | 0.8192 | 0.8403 | 0.8683 | 0.8974 | 0.9014 |
| 0.60 | 0.6649 | 0.6895 | 0.7124 | 0.7271 | 0.7376 | 0.7455 | 0.7601 | 0.7783 | 0.8013 | 0.8224 | 0.8236 |
| 0.80 | 0.5968 | 0.6202 | 0.6433 | 0.6588 | 0.6701 | 0.6788 | 0.6951 | 0.7150 | 0.7382 | 0.7560 | 0.7551 |
| 1.00 | 0.4455 | 0.4807 | 0.5196 | 0.5457 | 0.5648 | 0.5800 | 0.6080 | 0.6414 | 0.6771 | 0.7014 | 0.7007 |

Table 6: Normalized SIFs of three parallel cracks with same length in infinite plate reported by Isida (1976)

| a/d | 0.0 | 0.2 | 0.4 | 0.6 | 0.8 |
|---|---|---|---|---|---|
| $F_{IA}$ | 1.00000 | 0.98198 | 0.94010 | 0.89080 | 0.85052 |

parallel square-hole cracks shown in Fig.1 are almost equal to those corresponding to three parallel cracks with the same crack length and the same spacing.

The above two points illustrate that the numerical results obtained for three parallel square-hole cracks shown in Fig.1 are accurate and effective.

From Table 4, it can be seen that, for any $a/b$, variations of the normalized SIFs $F_{Ithcp}$ at the crack tip $A$ for three parallel square-hole cracks with $a/d$ are similar to those of the normalized SIFs $F_{Itcp}$ at the crack tip $A$ for three parallel cracks. For $a/b = 1.01, 1.10, 4.00$, for example, the SIFs $F_{Ithcp}$ at the crack tip $A$ are shown in Fig.7, from which the observation can be proven.

From Table 4, it can be also seen that, for any $a/d$, variations of the normalized SIFs $F_{Ithcp}$ of three parallel square-hole cracks with $a/b$ are similar to those of the normalized SIFs $F_{Ish}$ of a square hole crack. For $a/d = 0.05, 0.60, 1.0$, for example, the SIFs $F_{Ithcp}$ at the crack tip $A$ are shown in Fig.8, from which the observation can be proven.

Based on discussions on an effect of a square hole on a crack emanating from the square hole in an infinite plate subjected to internal pressure and the similarity of variations of the SIFs $F_{Ithcp}(a/b, a/d)$ with $a/b$ to that of the SIFs $F_{Ish}(a/b)$ with $a/b$, we come to conclude that there is also a shielding effect for three parallel square-hole cracks in an infinite plate subjected to internal pressure. The shielding effect perhaps has an important meaning in engineering. For example, suppose that there are three parallel cracks in an infinite plate subjected to internal pressure with $a/d = 0.80$. From Table 6, the normalized SIF is 0.85052. Here, suppose also that three parallel square holes are cut out on the three parallel cracks with $a/b = 1.02$. From Table 4, the normalized SIF is 0.7082. Thus it can be concluded from these data that the plate with the three parallel square-hole cracks with $a/b = 1.02$ is much safer than that with the three parallel cracks.

## 4 Conclusions

From the present investigations, the following conclusions can be made

By using the hybrid displacement discontinuity method, the interactions of three parallel square-hole cracks in an infinite plate subjected to internal pressure were investigated. The detail numerical results of the SIFs were given, from which it can be seen that

($a$) Variations of the SIFs $F_{Ithcp}(a/b, a/d)$ at the crack tip $A$ for three parallel square-hole cracks with $a/b$ are similar to those of the SIFs$F_{Ish}(a/b)$ of a square-hole crack with $a/b$. In particular, it is found that a square hole has a shielding effect on the cracks emanating from the hole and that the closer the size of the square hole is to that of the crack, the stronger the shielding effect is.

($b$) Variations of the SIFs $F_{Ithcp}(a/b, a/d)$ at the crack tip $A$ for three parallel square-hole cracks with $a/d$ are similar to those of the SIFs$F_{Itcp}(a/d)$ at the crack tip $A$ for three parallel cracks with $a/d$.

**Acknowledgement:** Special thanks are due to the National Natural Science Foundation of China (No.10272037 and No.10672046) for supporting the present work.

## References

**Aliabadi, M. H.** (1997): Boundary element formulation in fracture mechanics. *Applied Mechanics Review,* vol. 50, pp. 83-96.

**Blandford, G. E.; Ingraffea, A. R.; Liggett, J. A.** (1981): Two-Dimensional Stress Intensity Factor Computations Using the Boundary Element Method. *Int J. Num Methods Eng.,* vol. 17, pp. 387-404.

**Bowie, O. L.** (1956): Analysis of an infinite plate containing radial cracks originating at the boundary of an internal circular hole. *J. Math. Phys.,* vol. XXXV, no. 1, pp. 60-71.

**Crouch, S. L.; Starfied, A. M.** (1983): *Boundary Element Method in Solid Mechanics.* London, Geore Allon & Unwin, Bonton, Sydney.

**Cruse, T. A.** (1972): Numerical Evaluation of Elastic Stress Intensity Factors by Boundary Integral Equation Method, in "Surface Cracks Physics Problems and Computational Solutions". Swedlow J.L. (ed), ASME, New York, pp. 153-170.

**Cruse, T. A.** (1978): Two-dimensional BIE fracture mechanics analysis. *Appl. Math. Modelling,* vol. 2, pp. 287-293.

**Cruse, T. A.** (1989): *Boundary Element Analysis in Computational Fracture Mechanics.* Dordrecht: Kluwer, pp. 1-230.

**Dong, L.; Atluri, S. N.** (2012): SGBEM (Using Non-hyper-singular Traction BIE), and Super Elements, for Non-Collinear Fatigue-growth Analyses of Cracks in Stiffened Panels with Composite-Patch Repairs. *Computer Modeling in Engineering & Sciences,* vol. 89, no. 5, pp. 415-456.

**Dong, L.; Atluri, S. N.** (2013a): Fracture & Fatigue Analyses: SGBEM-FEM or XFEM? Part 1: 2D Structures. *CMES: Computer Modeling in Engineering & Sciences,* vol. 90, no. 2, pp. 91-146.

**Dong, L.; Atluri, S. N.** (2013b): Fracture & Fatigue Analyses: SGBEM-FEM or XFEM? Part 2: 3D Solids. *CMES: Computer Modeling in Engineering & Sciences,* vol. 90, no. 5, pp. 379-413.

**Isida, M.** (1976): Elastic analysis of cracks and stress intensity factors, Fracture

Mechanics and Strength of Materials 2, Baifuukan, pp. 193-201.

**Kebir, H.; Roelandt, J. M.; Foulquier, J.** (1999): A new singular boundary element for crack problems. *Application to bolted joints. Engineering Fracture Mechanics,* vol. 69, pp. 497-510.

**Leonel, E. D.; Venturini, W. S.** (2010): Boundary element formulation applied to analysis of multi-fractured domains. *Engineering Analysis with Boundary Elements,* vol. 34, pp. 1092-1099.

**Mi, Y.; Aliabadi, M. H.** (1992): Dual- boundary element method for three dimensional fracture mechanics analysis. *Eng. Ana. with Boundary Elements,* vol. 10, pp. 161-171.

**Murakami, Y.** (1978): A method of stress intensity factor calculation for the crack emanating from an arbitrarily shaped hole or the crack in the vicinity of an arbitrarily shape hole. *Trans. Japan Soc. Mech. Engrs,* vol. 44, no. 378, pp. 423-432.

**Newman, J. C. Jr.** (1971): An improved method of collocation for the stress analysis of cracked plates with various shaped boundaries, NASA TN, D-6376, pp. 1-45.

**Nisitani, K.; Isida, M.** (1982): Simple procedure for calculating $K_I$ of a notch with a crack of arbitrary size and its application to non-propagating fatigue crack, Proc. Ioint JSME-SESA Conf. On Experimental Mechanics, Part I, pp. 150-155.

**Park, J. H.; Atluri, S. N.** (1998): Mixed mode fatigue growth of curved cracks emanating from fastener holes in aircraft lap joints. *Computational mechanics,* vol. 21, no. 6, pp. 477-482.

**Portela, A.; Aliabadi, M. H.; Rook, D. P.** (1992): The dual boundary element method: effective implementation for crack problems. *Int. J. Num. Methods Eng.,* vol. 33, pp. 1269-1287.

**Tanaka, M.; Itoh, H.** (1987): New crack elements for boundary element analysis of elastostatics considering arbitrary stress singularities. *Appl Math Modelling,* vol. 11, pp. 357-363.

**Wang, H. T.; Yao, Z. H.** (2011): A fast multiple dual boundary element method for the three-dimensional crack problems. *Computer Modeling in Engineering & Sciences,* vol. 72, no. 2, pp. 115-147.

**Yan, X.** (2004a): A numerical analysis of perpendicular cracks under general in-plane loading with a hybrid displacement discontinuity method. *Mechanical Research Communications*, vol. 31, no. 2, pp. 175-183.

**Yan, X.** (2004b): A numerical analysis of cracks emanating from a square hole in a rectangular plate under biaxial loads. *Eng Fracture Mech.,* vol. 71, no. 11, pp. 1615-1623.

**Yan, X.** (2005a): Stress intensity factors for asymmetric branched cracks in plane extension by using crack tip displacement discontinuity elements. *Mechanics Research Communications,* vol. 32, no. 4, pp. 375-384.

**Yan, X.** (2005b): An effective boundary element method for analysis of crack problems in a plane elastic plate. *Appl Math Mech,* vol. 26, no. 6, pp. 814-822.

**Yan, X.** (2005c): Microdefect interacting with a finite main crack. *J Strain Analysis for Engineering Design*, vol. 40, no. 5, pp. 421-430.

**Yan, X.** (2006a): A numerical analysis of stress intensity factors at bifurcated cracks. *Engineering Failure Analysis,* vol. 13, no. 4, pp. 629-637.

**Yan, X.** (2006b): A numerical analysis of cracks emanating from an elliptical hole in a 2-D elasticity plate. *European J of Mechanics-A*, vol. 25, no. 1, pp. 142-153.

**Yan, X.** (2006c): A brief evaluation of approximation methods for microcrack shielding problems. ASME. *J. Appl. Mech.,* vol. 73, no. 4, pp. 694-696.

**Yan, X.** (2006d): Numerical analysis of stress intensity factor for two kinds of mixed-mode crack specimens. *J Strain Analysis for Engineering Design,* vol. 41, no. 1, pp. 9-18.

**Yan, X.** (2006e): Multiple crack fatigue growth modeling by displacement discontinuity method with crack-tip elements. *Appl Math Modeling,* vol. 30, no. 6, pp. 489-508.